

Surface Science Letters

Strong relaxations at the $\text{Cr}_2\text{O}_3(0001)$ surface as determined via low-energy electron diffraction and molecular dynamics simulations

F. Rohr ^a, M. Bäumer ^a, H.-J. Freund ^{a,*}, J.A. Mejias ^b, V. Staemmler ^b, S. Müller ^c,
L. Hammer ^c, K. Heinz ^c

^a Fritz-Haber-Institut der Max-Planck Gesellschaft, Faradayweg 4–6, 14195 Berlin, Germany

^b Lehrstuhl für Theoretische Chemie der Ruhr-Universität Bochum, Universitätsstr. 150, 44780 Bochum, Germany

^c Lehrstuhl für Festkörperphysik, Universität Erlangen-Nürnberg, Staudtstr. 7, 91058 Erlangen, Germany

Received 30 September 1996; accepted for publication 14 October 1996

Abstract

The surface structure of $\text{Cr}_2\text{O}_3(0001)$ was investigated by quantitative low-energy electron diffraction and molecular dynamic simulations. In qualitative agreement with each other, both methods indicate strong vertical relaxations at and near the surface. These relaxations are concomitant with a charge reduction and depolarization, which stabilize the surface, yielding energies close to those found for non-polar oxide surfaces with non-divergent surface potentials. The lateral arrangement of oxygen atoms is identical to that in the bulk, i.e. there are no lateral distortions to accommodate the strong interlayer relaxations. The latter extend deep into the surface, with the experimentally determined changes of the first four interlayer distances being -38% , -21% , -25% and $+11\%$ with respect to the unrelaxed bulk values.

Keywords: Chromium; Electron–solid interactions, scattering, diffraction; Insulating surfaces; Low energy electron diffraction (LEED); Surface energy; Surface structure, morphology, roughness, and topography

Polar surfaces of ionic oxides are inherently unstable due to the divergence of the electrostatic surface potential [1,2]. The divergence of the surface potential leads to massive reconstructions of the so-called octopolar type in the case of (111) surfaces of rock salt oxides, such as NiO [3,4]. In this case metal terminated and oxygen terminated (111) surfaces are structurally equivalent, therefore both terminations behave similarly with respect to structural changes. For corundum-type oxides

the situation is different. Fig. 1a shows a schematic representation of the stacking of layers along a direction perpendicular to the (0001) plane. Basically, flat oxygen layers alternate with buckled metal ion layers. If this stack of layers is cut between an oxygen plane and a buckled metal ion plane, one oxygen-terminated and one metal-ion-terminated surface are created. The metal-ion-terminated (0001) surface is plotted in Fig. 1b as a top view. Such a surface is electrostatically unstable due to the divergence of the surface potential. The situation may, however, be reconciled by cutting the stack of layers (Fig. 1a) not between the oxygen

*Corresponding author. Fax +49 30 8413 4101;
e-mail: freund@fhi-berlin.mpg.de

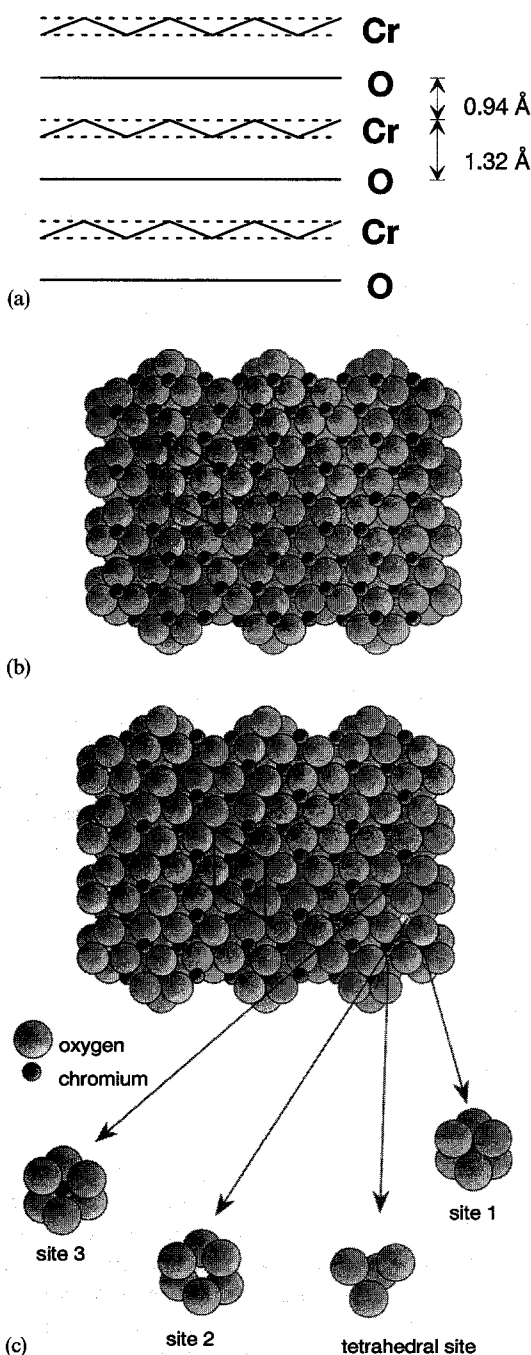


Fig. 1. (a) Schematic representation of the stacking of oxygen and chromium ions in Cr_2O_3 along the (0001) direction into the bulk volume. (b) Top view of the $\text{Cr}_2\text{O}_3(0001)$ surface terminated by a full Cr ion layer. (c) Depolarized $\text{Cr}_2\text{O}_3(0001)$ surface with half a layer of chromium ions.

and metal ion layers but rather in between the buckled metal ion layer, such that only half of the number of metal ions is left on each surface created. This surface is shown in Fig. 1c, as viewed from the top. The structure of this surface has been subject to a number of theoretical investigations, ranging from empirical pair potential treatments [5] to fully self-consistent ab initio studies both at the Hartree–Fock level [6] and via density functional methods [7]. The specific example treated theoretically most frequently has been the $\text{Al}_2\text{O}_3(0001)$ surface. It is expected that similar results would be obtained for other corundum-type surfaces, including transition metal oxides such as $\text{Cr}_2\text{O}_3(0001)$ [8] and $\text{Fe}_2\text{O}_3(0001)$. The main result of all calculations is a very pronounced relaxation of interlayer distances even though the surface is depolarized by the presence of only half of the number of metal ions in the surface. Ab initio calculations via density functional theory employing pseudopotentials [7] predict a very large relaxation of the last atomic plane of $\text{Al}_2\text{O}_3(0001)$ (–86%), while Hartree–Fock calculations yield a smaller value of –46% [6]. In some calculations, in-plane displacements of the oxygen atoms have been predicted [9]. These predictions have, so far, not been tested experimentally by electron energy diffraction due to charging of the insulating bulk material. Very recently, X-ray scattering from a bulk Al_2O_3 single crystal (0001) surface has been reported [10]. This study was performed under ultrahigh vacuum (UHV) conditions and surface composition was checked via Auger measurements. In line with the theoretical predictions, strong relaxations were deduced from the experimental data.

In the present study we report on the first study we report on the first study of a UHV stable transition metal oxide, namely $\text{Cr}_2\text{O}_3(0001)$, by quantitative and full dynamical low-energy electron diffraction (LEED). The $\text{Cr}_2\text{O}_3(0001)$ surface has been characterized with a series of different surface sensitive tools, including XPS, ARUPS, EELS, IRAS and ISS [11–16]. Unlike the $\text{Fe}_2\text{O}_3(0001)$ [17,18] surface, $\text{Cr}_2\text{O}_3(0001)$ is stable under ultrahigh vacuum conditions and can be studied at low temperatures with LEED if it is prepared as a thin epitaxial film of a thickness of

about 40 Å. We have complimented the experimental study and analysis of the $I(E)$ data by a molecular dynamics study, which allows us to compare predictions with experiments. We also find large relaxations, which are in part compatible with the X-ray analysis of the $\text{Al}_2\text{O}_3(0001)$ surface. The relaxations found experimentally and theoretically are in qualitative agreement. Furthermore, the simulations allow us, in particular, to explore alternative possibilities for the surface structure in order to get an idea of how stable the surface is on a relative scale. This comparison may be of importance in understanding the observed phase transition on $\text{Cr}_2\text{O}_3(0001)$ [15] when the surface is heated from 90 to 150 K.

The $\text{Cr}_2\text{O}_3(0001)$ film was prepared as described in detail in Refs. [11–16]. The polished chromium single crystal with a (110) oriented surface was cleaned by prolonged sputtering with argon at elevated temperatures, near 800 K, until no contamination with nitrogen could be detected. The oxide was prepared by exposure to 300 L of O_2 while linearly increasing the temperature to 780 K. After O_2 -dosage the sample was briefly flashed to 1000 K to facilitate ordering of the surface. Subsequently, a sharp and low background (1×1) LEED pattern was observed. Prior to each measurement the sample was cleaned by this flashing procedure at a base pressure of 5×10^{-11} Torr. The sample temperature was monitored by a Ni/CrNi thermocouple. In some cases the preparation conditions were slightly modified in order to check the reproducibility of the LEED data. In fact no variations in the data have been found.

LEED intensity versus energy $I(E)$ data were taken using a computer-controlled video LEED system, described in more detail in Refs. [19,20]. A conventional four grid reverse view LEED optics was used to perform the diffraction experiments. LEED spot intensities were recorded by means of a low-noise video camera. The video signal was accumulated, averaged and digitized by a frame grabber board. Data processing has been performed in an on-line fashion by software designed in-house. The program includes a spot search and track algorithm and routines for background subtraction and intensity integration. Data processing cycles are repeated at each particular

energy while the $I(E)$ spectra evolve. While the grabber board offers a maximum data acquisition speed determined by the video rate, the effective board speed is mostly governed by the averaging procedure and data transfer between board and computer CPU. Each $I(E)$ spectrum was recorded within 360 s. All $I(E)$ spectra were recorded with the sample cooled to 90 K at normal incidence of the primary electron beam and up to a maximum energy of 500 eV. According to the sixfold symmetry of the diffraction pattern, spectra of symmetrically equivalent beams could be averaged to improve the quality of data. Residual gas adsorption during data acquisition was not observed to influence the $I(E)$ data.

Molecular dynamics simulations were performed in the isobaric isothermal ensemble by employing the method of Parinello and Rahman [21]. We assume a completely ionic model and the forces applied to atoms were derived from pair potentials, which include electrostatic interactions (between formal charges +3, and -2), short-range repulsion ($A \exp(-BR)$), O–O dispersion (D/r^6) as well as Cr–O and O–O polarization terms (C/r^4). The interaction parameters A , B and D are taken from the work by Lawrence et al. [22], and the polarization terms are chosen to reproduce crystal energy, lattice parameters and phonon frequencies of the Cr_2O_3 bulk. We have used slab models with 1470, 2430 and 3240 particles. The slabs are periodic in three dimensions, with a void of approximately 140 Å between periodic images perpendicular to the surface. All molecular dynamics simulations were done with the program MOLDY [23]. The time step was 1 fs and the velocities were scaled during 5 ps before production runs of 20 ps. The time evolution was followed at several temperatures (7, 150 and 300 K).

The full dynamical LEED analysis was performed in two steps: first, standard computer programs [24,25] were applied to retrieve the rough structural features, i.e. the sites of the top metal atoms and the interlayer distances. This was done by testing four possible sites (see below) and applying a grid search in each case for the vertical interlayer distances. In a second step, the best-fit model found in step 1 was refined using the perturbation method tensor-LEED [26–28] and an

automized structural search procedure [29], which also allowed for lateral atomic shifts. The validity of the eventually found best-fit structure was confirmed by a final full dynamical calculation. The Pendry R -factor [30] was used for the quantitative comparison of the experimental and calculated spectra, guiding the structural search. Error limits for the structural parameters were retrieved from the variance of the R -factor. The intensity calculations were restricted to a maximum electron energy of 300 eV, leaving a total data base width of 1000 eV. This is, on the one hand, to save computer time and on the other to allow the layer doubling procedure to be applied for the stacking of composite layers with distances as small as 0.94 Å. As many as 499 symmetrically non-equivalent beams were used in the layer stacking procedure. The layers were composite layers with two oxygen sublayers and two chromium double layers, i.e. with ten and nine atoms in the unit cells of bulk and surface composite layers, respectively. Their diffraction was calculated in angular momentum representation by matrix inversion allowing for any degree of intersublayer relaxation. We emphasize that the treatment of several of such large and thick composite layers is a demanding task even when powerful computers are at hand and this makes the present LEED analysis largely non-routine. Five of such 3.59 Å thick composite layers were stacked, which (according to their cumulated width of 14.39 Å) made consideration of the underlying bulk unnecessary due to electron attenuation. The latter was simulated through an imaginary part of the inner potential as usual (best fit value: 4.5 eV). The atomic scattering was described by eight relativistically calculated and spin-averaged phase shifts for the two elements, corrected for thermal vibrations, which were assumed to be isotropic, and using Debye temperatures of 91 and 630 K for oxygen and chromium, respectively [31].

In the introduction we alluded to the metal-ion-terminated surface with only half of the ions present in the topmost layer. In Fig. 1c, one of the several possible sites for the chromium ions, namely the one that corresponds to the bulk position, has been artificially chosen. It is quite conceivable that other positions can be occupied. In principle there

are four different positions available. These are marked as 1, 2, 3 and t (tetrahedral) in Fig. 1c. The site corresponding to the bulk situation is position 2. In order to perform an $I(E)$ analysis it is important to have an idea of the relative stability of the surface if different sites are occupied in the terminating metal ion layer. Table 1 collects the surface energies for the different sites as evaluated by Marvin's program [32] with full ionic pair potentials.

It is interesting to note that the surface with the lowest surface energy is that with the chromium site occupied according to the bulk situation. Starting from different configurations in which sites 1, 2, 3 and t had been initially occupied, and independent of temperature, all chromium ions occupied site 2 after equilibration had been achieved. The energy is comparable with the most stable non-polar rock salt surfaces of NiO, for example. The NiO(100) surface has an energy of 1.38 J m^{-2} . However, while the rock salt surfaces are only weakly relaxed [2], the molecular dynamics simulations indicate rather pronounced relaxations of the interlayer spacing in the present case. Also, very recently Hartree–Fock calculations [8] on the $\text{Cr}_2\text{O}_3(0001)$ surface have been reported and strong relaxations are predicted. In Table 2, together with Fig. 2, the relaxations calculated for the $\text{Cr}_2\text{O}_3(0001)$ surface via the molecular dynamics simulation as well as via the Hartree–Fock calculations are compared. Table 2 also contains the available information on the corresponding $\text{Al}_2\text{O}_3(0001)$ surface.

The predicted relaxations alternate and reach from the surface to about five layers down into the solid. All theoretical results indicate a strong inward relaxation of the top chromium ion layer. This is expected because the chromium ions in the

Table 1
Surface energies for various sites of chromium ions on the surface; for assignment see Fig. 1c

Site	$E_{\text{surf}} (\text{J m}^{-2})$
1	4.36
2	1.60
3	6.34
t	2.69

Table 2
Surface relaxations (%) of bulk interlayer distances^a

System	a	b	c	d	Ref.
Cr₂O₃					
MD simul.	-58	0	-36	+17	This work
HF calc.	-50	+3.3	0	0	[8]
LEED	-38±4	-21±6	-25±16	+11±9	This work
Al₂O₃					
DFT calc.	-86	+3	-54	+25	[7]
HF calc.	-46	Not given			[6]
Empirical slab	-65	-5	-32	+14	[33]
Empirical semi-infi	-59	+2	-49	+26	[5]
X-ray	-51	+16	-29	+20	[10]

^a Cr–O interlayer distance: 0.94 Å, Al–O interlayer distance: 0.84 Å, Cr–Cr interlayer distance: 0.39 Å, Al–Al interlayer distance: 0.485 Å. For a, b, c and d see schematic drawing in Fig. 2.

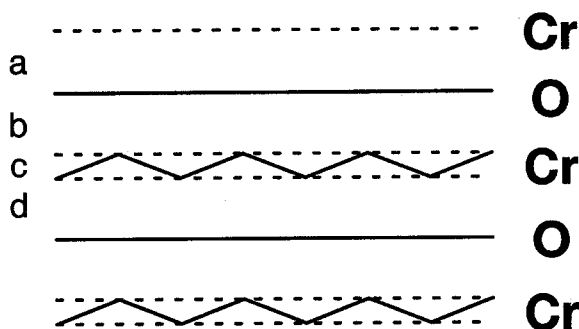


Fig. 2. Schematic representation of the stacking of layers with respect to the depolarized surface.

top layer miss half of the oxygen ions and are, therefore, electrostatically attracted into the surface. Interestingly, there is no significant lateral shift of the oxygen ions in the surface, indicating that the chromium ions are sufficiently small so as to avoid Pauli repulsion with the oxygen ion cores even after an inward relaxation of 50–60%. Also, there is no indication from the calculations of a significant change of the ionicity in the surface as compared with the bulk. While this is not surprising in the case of Al₂O₃, because aluminium does not have a strong tendency to change its valence state, such an effect might be expected for chromium. However, the available Hartree–Fock calculations [8] predict, basically, a conservation of the bond character between chromium and oxygen, and, if anything, a very slight lowering of the

ionicity of the chromium ions in the top layer. In the MD simulations for Cr₂O₃, a change in the ionicity cannot be accounted for as full ionic charges have been used both for bulk and surface ions. The high ionicity is also responsible for the fact that the relaxation of the top Cr–O layer distance is larger in the theoretical simulation than in the experimental geometry. The predicted relaxations of deeper layers differ quantitatively and in sign, depending on the calculation. In most calculations the distance between the top oxygen layer and the second chromium layer increases by a few percent, but there are also predictions of a slight contraction of this interlayer distance. Again, all calculations predict a strong smoothing of the buckling of the second full metal ion layer. The Hartree–Fock calculations on Cr₂O₃ do not seem to have taken this into account. The next chromium–oxygen interlayer distance into the volume of the material is contracted with respect to the bulk situation. In summary, the contractions and expansions of the interlayer distances alternate when going from the surface into the volume. In this respect the situation is basically similar to metal surfaces, where similar alternative relaxations are found. However, in the case of polar surfaces of ionic oxide materials it seems that the magnitude of the effects are considerably more pronounced as compared with metal surfaces. This is, in fact, not too surprising because, in the case of metals, screening due to the presence of the

metal electrons helps to damp the oscillatory behaviour. The more localized electronic structure of dielectric materials does not support this electronic damping and thus the strong electrostatic interactions are fully revealed by the geometric structure.

The quantitative analysis of the LEED data yields best-fit R -factors for sites 1, 2, 3 and the t -site of 0.62, 0.32, 0.68 and 0.55, respectively. By the variance of the R -factor, $\text{var}(R)=0.057$, sites 1, 3 and t can be definitely excluded. The overall best-fit spectra for site 2 are compared with the experimental data in Fig. 3, showing apparently good agreement. The best-fit interlayer relaxations together with the theoretical predictions are given in Table 2, including the error limits as found by the variance of the R -factor. The errors increase with depth because of electron attenuation and are particularly high for the small distance within the

chromium double layer (note that the absolute errors for layer distances a – d are 0.04, 0.06, 0.09 and 0.09 Å, respectively). The arrangement of the oxygen ions within the oxygen layers is almost identical with that in the bulk. In particular, there are no lateral distortions. Except for the strong contraction of the second chromium–oxygen interlayer distance, the results are consistent with the predictions. Firstly, the predicted contraction of the top interlayer distance is, indeed, revealed by the measurements. Secondly, the relaxation reaches well into the volume of the material. The present experiments, however, indicate that both the top chromium–oxygen interlayer distance, as well as the second chromium–oxygen interlayer distances contract. The buckling of the subsurface layer of chromium ions is smoothed and the next chromium–oxygen distance down in the bulk is enlarged. The result of the surface relaxation is a separation of the top Cr–O–Cr unit of layers from the bulk. This may have consequences for the electronic structure near the surface and should be explored theoretically in the future.

The structural relaxations revealed in this study have consequences with respect to the interpretation of the electronic excitations discussed in the literature. On the basis of electronic EELS data and *ab initio* calculations [15] the site for the chromium ions in the surface has been assigned. The calculations were based on the unrelaxed geometry of the surface, and it was indicated that the final assignment would depend on a detailed knowledge of the geometry, because considerable changes in the ligand field at the chromium positions are to be expected if the chromium ions relax into the oxygen layer, and consequently the d – d excitations will change in energy. We have repeated the quantum chemical *ab initio* calculation for the d – d excitation energies of Cr^{3+} ions occupying site 2 at the relaxed $\text{Cr}_2\text{O}_3(0001)$ surface. The excitation energies are 0.99, 1.25, 1.42 and 1.62 eV for the surface structure, as obtained by molecular dynamics, and 0.75, 1.10, 1.30 and 1.40 eV for the experimental geometry. Given an uncertainty of 0.1 eV in the calculated excitation energies, the data are in reasonable agreement with the two prominent surface excitations at 1.24 and 1.40 eV in the experimental EELS spectrum [15].

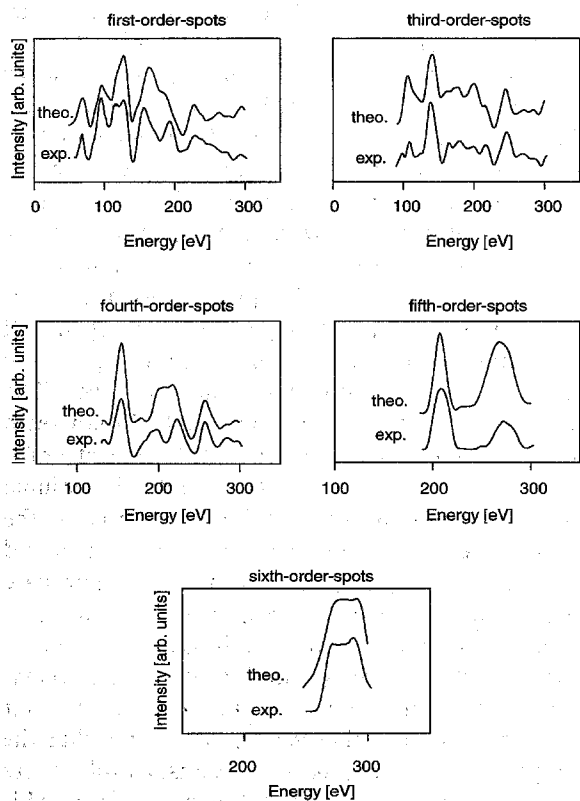


Fig. 3. Comparison of measured $I(E)$ curves with theoretical fits.

Therefore, the assignment of site 2 instead of site 1, which was the proposed site according to Ref. [15], is compatible with the present data.

In summary, we have presented the first full $I(E)$ LEED study of a thermodynamically stable, depolarized $\text{Cr}_2\text{O}_3(0001)$ surface. This surface is a prototype for transition metal oxides of corundum-type structure. The surface is chromium terminated and the interlayer distances are strongly relaxed. The top chromium–oxygen interlayer distance contracts by about 38%. Also, the following two interlayer distances contract by more than 20% (21 and 25%). Only the third interlayer distance enlarges (by 11%). Thus, the relaxation reaches down five to six layers into the volume. The experimentally determined relaxations are in qualitative agreement with predictions from a molecular dynamics simulation. This simulation also predicted, in harmony with the experimental data, site 2 (in Fig. 1c) as the most stable site in the surface for the chromium ions. The surface energy of the relaxed $\text{Cr}_2\text{O}_3(0001)$ surface has been calculated to be 1.6 J m^{-2} , which is rather close to the energy of a non-polar $\text{NiO}(100)$ surface.

Acknowledgements

This work has been supported by Deutsche Forschungsgemeinschaft, Ministerium für Wissenschaft und Forschung des Landes Nordrhein-Westfalen, and Fonds der Chemischen Industrie.

References

- [1] J.W. Tasker, *J. Phys. C* 12 (1979) 4977; *Philos. Mag. A* 39 (1979) 119.
- [2] H.-J. Freund, H. Kuhlenbeck and V. Staemmler, *Rep. Progr. Phys.* 59 (1996) 283.
- [3] D. Wolf, *Phys. Rev. Lett.* 68 (1992) 3315.
- [4] F. Rohr, K. Wirth, J. Libuda, D. Cappus, M. Bäumer and H.-J. Freund, *Surf. Sci.* 315 (1994) L977.
- [5] W.C. Mackrodt, R.J. Davey, S.N. Black and R. Docherty, *J. Cryst. Growth* 80 (1987) 441.
- [6] M. Causa, R. Dovesi, C. Pisani and C. Roetti, *Surf. Sci.* 215 (1989) 259.
- [7] I. Manassidis and M.J. Gillan, *Surf. Sci.* 285 (1993) L517.
- [8] C. Rehbein, N.M. Harrison and A. Wander, to be published.
- [9] T.J. Godin and J.P. LaFemina *Phys. Rev. B* 49 (1994) 7691.
- [10] P. Guenard, G. Renaud, A. Barbier and M. Gautier-Soyer, *Proc. ICSOS, Aix-en-Provence* (1996).
- [11] C. Xu, B. Dillmann, H. Kuhlenbeck and H.-J. Freund, *Phys. Rev. Lett.* 67 (1991) 3551.
- [12] C. Xu, M. Haßel, H. Kuhlenbeck and H.-J. Freund, *Surf. Sci.* 258 (1991) 25.
- [13] H. Kuhlenbeck, C. Xu, B. Dillmann, M. Haßel, B. Adam, D. Ehrlich, S. Wohlrab, H.-J. Freund, U.A. Ditzinger, H. Neddermeyer, M. Neuber and M. Neumann, *Ber. Bunsenges. Phys. Chem.* 96 (1992) 15.
- [14] C.A. Ventrice, D. Ehrlich, E.L. Garfunkel, B. Dillmann, D. Heskett and H.-J. Freund, *Phys. Rev. B* 46 (1992) 12892.
- [15] M. Bender, D. Ehrlich, I.N. Yakovkin, F. Rohr, M. Bäumer, H. Kuhlenbeck, H.-J. Freund, V. Staemmler, *J. Phys. C* 7 (1995) 5289.
- [16] B. Dillmann, O. Seiferth, G. Klivenyi, F. Rohr, I. Hemmerich, M. Bender, I. Yakovkin, D. Ehrlich and H.-J. Freund, *Faraday Disc., Chem. Soc.* (1996), to be published.
- [17] N.G. Condon, R.W. Murray, F.M. Leibsle, G. Thornton, A.R. Lemic and J. Vaughan, *Surf. Sci.* 310 (1994) L609.
- [18] T. Schedel-Niedrig, W. Weiß and R. Schlögl, *Phys. Rev. B* 52 (1995) 17449.
- [19] K. Wirth, *Diplomarbeit, Ruhr-Universität Bochum*, 1993.
- [20] F. Rohr, *Thesis, Ruhr-Universität Bochum*, in preparation.
- [21] M. Parinello and R. Rahman, *J. Appl. Phys.* 52 (1981) 7182.
- [22] P.J. Lawrence, S.C. Parker and P.W. Tasker, *Adv. Ceram.* 23 (1987) 247.
- [23] *MOLDY Revision 2.10* by K. Refson.
- [24] M.A. Van Hove and S.Y. Tong, *Surface Crystallography by LEED* (Springer, Berlin, 1979).
- [25] J.B. Pendry, *Low Energy Electron Diffraction* (Academic Press, London, 1974).
- [26] P.J. Rous, J.B. Pendry, D.K. Saldin, K. Heinz, K. Mueller and N. Bickel, *Phys. Rev. Lett.* 57 (1986) 2951.
- [27] P.J. Rous and J.B. Pendry, *Surf. Sci.* 219 (1989) 355; 373.
- [28] P.J. Rous, *Progr. Surf. Sci.* 39 (1992) 3.
- [29] M. Kottcke and K. Heinz, *Surf. Sci.*, submitted.
- [30] J.B. Pendry, *J. Phys. C* 13 (1980) 937.
- [31] *American Institute of Physics Handbook*, Ed. E. Gray (McGraw-Hill, New York, 1972).
- [32] *Marvins's Version 1.65* by D. Gay and A. Rohl.
- [33] C.R.A. Catlow, R. James, W.C. Mackrodt and R.F. Stewart, *Phys. Rev. B* 25 (1982) 1006.